

# Spontaneous spin current near the interface between unconventional superconductors and ferromagnets

Kazuhiro Kuboki and Hidenori Takahashi

*Department of Physics, Kobe University, Kobe 657-8501, Japan*

(October 29, 2018)

We study theoretically the proximity effect between ferromagnets (F) and superconductors (S) with broken time-reversal symmetry ( $\mathcal{T}$ ). A chiral  $(p_x \pm ip_y)$ -wave, and a  $d_{x^2-y^2}$ -wave superconductor, the latter of which can form  $\mathcal{T}$ -breaking surface state, i.e.,  $(d_{x^2-y^2} \pm is)$ -state, are considered for the S side. The spatial variations of the superconducting order parameters and the magnetization are determined by solving the Bogoliubov de Gennes equation. In the case of a chiral  $(p_x \pm ip_y)$ -wave superconductor, a spontaneous spin current flows along the interface, but not in the case of a  $d_{x^2-y^2}$ -wave superconductor. For F/S( $p_x \pm ip_y$ )/F trilayer system, total spin current can be finite while total charge current vanishes, if the magnetization of two F layers are antiparallel.

PACS numbers: 74.45.+c, 74.50.+r, 74.78.Fk

## I. INTRODUCTION

Recently the proximity effect of unconventional superconductors has been a subject of intensive study [1–8]. This is because the interface properties of these superconductors can be quite different from those of conventional ( $s$ -wave) ones due to the nontrivial angular structure of pair wave functions, so that their study is of particular interest. The proximity effect between unconventional superconductors and magnetic materials is an important problem, since there are competition and the possible coexistence of two kinds of orders. The unconventional superconductivity is usually induced by the magnetic interaction, and the existence of nodes in the gap is favorable for the coexistence compared with the case of conventional superconductors. If the magnetism and superconductivity coexist near the interface, the electronic properties of the surface state become quite unusual. In particular the spin-triplet superconducting order parameter (SCOP) can be induced near the surface of spin-singlet superconductors [5]. (Similar effects for conventional  $s$ -wave superconductors and ferromagnets have been studied in [9–11].)

In this paper we study the proximity effect between ferromagnets and unconventional superconductors with  $d_{x^2-y^2}$ -wave and  $(p_x \pm ip_y)$ -wave symmetries. The former state is realized in high- $T_c$  cuprates [12], while the latter is a candidate of the superconducting (SC) state of  $\text{Sr}_2\text{RuO}_4$  [13]. It is known that near the [110] surface of the  $d_{x^2-y^2}$ -wave superconductor the system may break time-reversal symmetry ( $\mathcal{T}$ ) by introducing second component of SCOP [14–18,7,8], and that a spontaneous current and fractional vortices may occur at the surface if  $\mathcal{T}$  is broken [19–21,14–18,7,8]. The  $(p_x \pm ip_y)$ -wave SC states also break  $\mathcal{T}$  and the spontaneous current arises at the edge of the system [22]. When a ferromagnet is attached to these unconventional superconductors, the magnetization may be induced in the latter due to the

proximity effect [5]. Then it may be expected that a spontaneous spin current can appear along the interface between a  $\mathcal{T}$ -breaking superconductor and a ferromagnet, because there is an imbalance of the densities of spin-up and spin-down electrons. We will show that it is actually possible for the superconductor with  $(p_x \pm ip_y)$ -wave symmetry, but not in the case of  $d_{x^2-y^2}$ -wave symmetry [23]. (Spin currents in the case of interfaces between  $s$ -wave superconductors and ferromagnets have been found in [24], though their treatment of the magnetization is not fully self-consistent.)

## II. MODEL AND BDG EQUATIONS

The system we consider is a two-dimensional ferromagnet(F)/superconductor(S) bilayer and F/S/F trilayer systems, and we treat [100] and [110] interfaces as schematically depicted in Fig.1. The directions perpendicular (parallel) to the interfaces are denoted as  $x$  ( $y$ ) and  $x'$  ( $y'$ ), for [100] and [110] interfaces, respectively. The axes  $x'$  and  $y'$  are  $45^\circ$  rotated from the crystal axes directions  $x$  and  $y$ . We assume that the system is uniform along the direction parallel to the interface. In order to describe the magnetism and superconductivity, the tight-binding model on a square lattice with on-site repulsive and nearest-neighbor attractive interactions is treated within the mean-field (MF) approximation [5,6], and we consider only the case of zero temperature ( $T = 0$ ). The Hamiltonians for the two layers are given by

$$H_L = -t_L \sum_{\langle i,j \rangle} (c_{i,\sigma}^\dagger c_{j,\sigma} + h.c.) + U_L \sum_i n_{i\uparrow} n_{i\downarrow} + V_L \sum_{\langle i,j \rangle} [n_{i\uparrow} n_{j\downarrow} + n_{i\downarrow} n_{j\uparrow}], \quad (L = F, S) \quad (1)$$

where  $\langle i, j \rangle$  denotes the nearest-neighbor bonds,  $n_{i\sigma} \equiv c_{i\sigma}^\dagger c_{i\sigma}$ , and  $c_{i\sigma}$  is the annihilation operator of electrons at a site  $i$  with spin  $\sigma$ . Parameters  $t_L$ ,  $U_L$  and  $V_L$

represent the transfer integral, the on-site interaction and the nearest-neighbor interaction, respectively, for the  $L(= F, S)$  side. The transmission of electrons at the interface is described by the following tight-binding Hamiltonian

$$H_T = -t_T \sum_{\langle l, m \rangle \sigma} (c_{l, \sigma}^\dagger c_{m, \sigma} + h.c.) \quad (2)$$

where  $l$  ( $m$ ) denotes the surface sites of  $F$  ( $S$ ) layer, and then the total Hamiltonian of the system is  $H = H_F + H_S + H_T - \mu \sum_{i \sigma} c_{i \sigma}^\dagger c_{i \sigma}$  with  $\mu$  being the chemical potential. The interaction terms are decoupled within the MF approximation:

$$\begin{aligned} U n_{i \uparrow} n_{i \downarrow} &\rightarrow U \langle n_{i \uparrow} \rangle n_{i \downarrow} + U \langle n_{i \downarrow} \rangle n_{i \uparrow} - U \langle n_{i \uparrow} \rangle \langle n_{i \downarrow} \rangle, \\ V n_{i \uparrow} n_{j \downarrow} &\rightarrow V \Delta_{ij} c_{j \downarrow}^\dagger c_{i \uparrow}^\dagger + V \Delta_{ij}^* c_{i \uparrow} c_{j \downarrow} - V |\Delta_{ij}|^2 \end{aligned} \quad (3)$$

with  $\Delta_{ij} \equiv \langle c_{i \uparrow} c_{j \downarrow} \rangle$ . Then  $\Delta_{ij}$  and the magnetization  $m_i = \langle n_{i \uparrow} - n_{i \downarrow} \rangle / 2$  (perpendicular to the plane) are the OP's to be determined self-consistently. The SCOP with each symmetry can be formed by combining  $\Delta_{ij}$ 's:  $\Delta_d(i) \equiv (\Delta_{i, i+\hat{x}}^{(S)} + \Delta_{i, i-\hat{x}}^{(S)} - \Delta_{i, i+\hat{y}}^{(S)} - \Delta_{i, i-\hat{y}}^{(S)}) / 4$  ( $d_{x^2-y^2}$ -wave),  $\Delta_s(i) \equiv (\Delta_{i, i+\hat{x}}^{(S)} + \Delta_{i, i-\hat{x}}^{(S)} + \Delta_{i, i+\hat{y}}^{(S)} + \Delta_{i, i-\hat{y}}^{(S)}) / 4$  (extended  $s$ -wave),  $\Delta_{px(y)}(i) \equiv (\Delta_{i, i+\hat{x}(y)}^{(T)} - \Delta_{i, i-\hat{x}(y)}^{(T)}) / 2$  ( $p_{x(y)}$ -wave), where  $\Delta_{ij}^{(S)} \equiv (\Delta_{ij} + \Delta_{ji}) / 2$  and  $\Delta_{ij}^{(T)} \equiv (\Delta_{ij} - \Delta_{ji}) / 2$  are the spin-singlet and the spin-triplet pairing OP's, respectively.

We impose the open (periodic) boundary condition for the  $x$  and  $x'$  ( $y$  and  $y'$ ) directions for [100] and [110] interfaces, respectively, and carry out the Fourier transformation along the  $y$ - and  $y'$ -directions. For the [100] case we define  $\Delta_{x_i}^{\pm} = \Delta_{i, i \pm \hat{x}}$  and  $\Delta_{x'_i}^{\pm} = \Delta_{i, i \pm \hat{y}}$  as the SCOP's independent of  $y$ . Similarly for the [110] case,  $\Delta_{x'_i}^{\alpha\beta} = \Delta_{i, i + \alpha \frac{\hat{x}'}{2} + \beta \frac{\hat{y}'}{2}}$  ( $\alpha, \beta = +$  or  $-$ ) are SCOP's independent of  $y'$ . ( $|\hat{x}| = |\hat{y}| = a$ ,  $|\hat{x}'| = |\hat{y}'| = a'$  with  $a$  and  $a'$  defined in Fig.1.) Then the mean-field Hamiltonian is written as (hereafter  $i$  denotes  $x_i$  and  $x'_i$  for a [100] and a [110] interface, respectively)

$$\mathcal{H}_{\text{MFA}} = \sum_k \sum_i \sum_j \Psi_i^\dagger(k) \hat{h}_{ij}(k) \Psi_j(k) \quad (4)$$

with  $\Psi_i^\dagger(k) = (c_{i \uparrow}^\dagger(k), c_{i \downarrow}^\dagger(-k))$ , and  $k$  is the wave number for the direction parallel to the interface. The matrix  $\hat{h}_{ij}(k)$  is given as

$$\hat{h}_{ij}(k) = \begin{pmatrix} \xi_{ij \uparrow}(k) & F_{ij}(k) \\ F_{ij}^*(k) & -\xi_{ij \downarrow}(k) \end{pmatrix}, \quad (5)$$

where

$$\begin{aligned} \xi_{ij \sigma}(k) &= (-2t_{ij} \cos ka - \mu + U \langle n_{i, -\sigma} \rangle) \delta_{ij} \\ &\quad - t_{ij} (\delta_{i, j+a} + \delta_{i, j-a}), \\ F_{ij}(k) &= V_{ij} [\Delta_i^{x+} \delta_{i, j-a} + \Delta_i^{x-} \delta_{i, j+a} \\ &\quad + (\Delta_i^{y+} e^{ika} + \Delta_i^{y-} e^{-ika}) \delta_{i, j}] \end{aligned} \quad (6)$$

for the [100] interface, and

$$\begin{aligned} \xi_{ij \sigma}(k) &= (-\mu + U \langle n_{i, -\sigma} \rangle) \delta_{ij} \\ &\quad - 2t_{ij} \cos\left(\frac{ka'}{2}\right) (\delta_{i, j+\frac{a'}{2}} + \delta_{i, j-\frac{a'}{2}}) \\ F_{ij}(k) &= V_{ij} [\delta_{i, j-\frac{a'}{2}} (\Delta_i^{++} e^{ika'/2} + \Delta_i^{+-} e^{-ika'/2}) \\ &\quad + \delta_{i, j+\frac{a'}{2}} (\Delta_i^{-+} e^{ika'/2} + \Delta_i^{--} e^{-ika'/2})] \end{aligned} \quad (7)$$

for the [110] interface. Here  $t_{ij} = t_{F(S)}$ ,  $V_{ij} = V_{F(S)}$  if both  $i$  and  $j$  are on the  $F$  ( $S$ ) side, while  $t_{ij} = t_T$ ,  $V_{ij} = 0$  if  $i$  and  $j$  correspond to the interface sites.

We diagonalize the mean-field Hamiltonian by solving the following Bogoliubov de Gennes (BdG) equation [25]:

$$\sum_j \hat{h}_{ij}(k) \begin{pmatrix} u_{jn}(k) \\ v_{jn}(k) \end{pmatrix} = E_n(k) \begin{pmatrix} u_{in}(k) \\ v_{in}(k) \end{pmatrix} \quad (8)$$

where  $E_n(k)$  and  $(u_{in}(k), v_{in}(k))$  are the energy eigenvalue and the corresponding eigenfunction, respectively, for each  $k$ . The unitary transformation using  $(u_{in}(k), v_{in}(k))$  diagonalizes the matrix  $\mathcal{H}_{\text{MFA}}$ , and conversely the OP's  $\Delta_{ij}$  and  $m_i$  can be written in terms of  $E_n(k)$  and  $(u_{in}(k), v_{in}(k))$ :

$$\begin{aligned} \Delta_i^{\pm} &= \frac{1}{N_y} \sum_{k, n} u_{i, n}(k) v_{i \pm a, n}^*(k) [1 - f(E_n(k))] \\ \Delta_i^{y \pm} &= \frac{1}{N_y} \sum_{k, n} u_{i, n}(k) v_{i, n}^*(k) [1 - f(E_n(k))] e^{\mp ika} \\ \Delta_i^{\alpha\beta} &= \frac{1}{N_{y'}} \sum_{k, n} u_{i, n}(k) v_{i + \alpha \frac{a'}{2}, n}^*(k) [1 - f(E_n(k))] e^{-i\beta ka'/2} \\ \langle n_{i \uparrow} \rangle &= \frac{1}{N_y} \sum_{k, n} |u_{i, n}(k)|^2 f(E_n(k)) \\ \langle n_{i \downarrow} \rangle &= \frac{1}{N_y} \sum_{k, n} |v_{i, n}(k)|^2 [1 - f(E_n(k))] \end{aligned} \quad (9)$$

where  $f(E)$  is the Fermi distribution function. (For the [110] case,  $N_y$  in the last two expressions should be replaced by  $N_{y'}$ .) These constitute the self-consistency equations which will be solved numerically in the following.

The procedure of the self-consistent numerical calculation is the following. We substitute an initial set of OP's in the matrix elements of  $\hat{h}_{ij}(k)$ , and solve BdG equation (Eq.(8)) to get eigenvalues and eigenfunctions. Then we recalculate the OP's, and the iteration is performed until the values of OP's are converged. We have used various sets of initial OP's for the same values of the parameters of the model. If several different solutions are obtained,

we adopt the solution with the lowest energy as the true one.

In the uniform case with  $U > 0$  and  $V = 0$  (i.e., repulsive Hubbard model), the ground state phase diagram within the MF approximation was examined by Hirsch [26]. We use this result to choose the parameters to realize the ferromagnetic state in the F layer. The phase diagram in the case of  $U = 0$  and  $V < 0$  was also studied, and the  $d_{x^2-y^2}$ -, extended  $s$ - and  $(p_x \pm ip_y)$ -wave SC state appears depending on the band filling [27]. Various SC states can occur in the model with a single type of (nearest-neighbor attractive) interaction because of the change of the shape of the Fermi surface [28]. Near half-filling ( $\mu \sim 0$ ) the  $d_{x^2-y^2}$ -wave SC state is stabilized, while the extended  $s$ -wave SC state is favored near the band edge ( $\mu \sim \pm 4t$ ). In the region between  $d$ - and  $s$ -wave states spin-triplet  $(p_x \pm ip_y)$ -wave SC state appears.

The properties of the interface states do not depend on the values of the parameters in a qualitative way, unless the symmetries of the superconducting ( $d_{x^2-y^2}$  or  $(p_x \pm ip_y)$ -wave) and the magnetic (ferromagnetic or antiferromagnetic) states are changed. Therefore we will choose typical values of the parameters in order to realize the states in question. We will use finite values of  $U_F$  to investigate the effect of electron correlations in the S side, while the attractive interaction in the F side is assumed to be absent, i.e.,  $V_F = 0$ . Hereafter we take  $t_F = t_S (\equiv t) = 1$  as the unit of energy, and the tunneling matrix element  $t_T$  is varied to see how the extent of the proximity effect is changed.

### III. INTERFACE STATES AND SPONTANEOUS SPIN CURRENTS FOR CHIRAL P-WAVE SUPERCONDUCTORS

In this section we study the proximity effect between ferromagnets and superconductors with  $(p_x \pm ip_y)$ -wave symmetry. Here the parameters are chosen to realize the ferromagnetic and  $(p_x \pm ip_y)$ -wave SC states in F and S layers, respectively, i.e.,  $U_F = 12$ ,  $V_S = -2.5$  and  $\mu = -1.6$ . The system size we used is  $N_x = N_y = 120$ , which is large enough to study the interface states, because the coherence lengths of SC and ferromagnetic states are of the order of  $10a$  for the parameters used here. The spatial variations of the SCOP's and the magnetization  $m$  near the [100] interface are shown in Fig.2 where the tunneling matrix element is taken to be  $t_T = 1$ , and  $U_S = 1.5$ . It is seen that  $\Delta_{px}$  and  $\Delta_{py}$  are suppressed near the interface, and the spin-singlet components  $\Delta_d$  and  $\Delta_s$  are induced. Near a surface of a chiral superconductor faced to vacuum, the spin-singlet components are not induced, though the  $p$ -wave SCOP's are suppressed also in this case [22]. This difference is due to the presence of  $m$  in the S side, because the SC state cannot be formed with  $(p_x \pm ip_y)$ -channel only, if  $\langle n_\uparrow \rangle \neq \langle n_\downarrow \rangle$ . The

proximity effects will be reduced as the tunneling matrix element becomes smaller. This is actually the case as seen in Fig.3 where  $t_T = 0.1$  is used. It is seen that the penetration of  $m$  into the S side is suppressed, and  $d$ - and  $s$ -wave SCOP's are much smaller compared with Fig.2. The change of the surface states, as  $t_T$  is varied, is rather simple in the case of  $(p_x \pm ip_y)$ -wave superconductors. Namely, the state monotonously approaches that for  $t_T = 0$  as  $t_T$  is reduced. (On the contrary, the surface state of a  $d$ -wave superconductor shows a phase transition when  $t_T$  is varied, as we will see in the next section.) The penetration depth of  $m$  depends on the electron correlation in the S side. The spatial variations of OP's for  $U_S = 5$  and  $t_T = 1$  are shown in Fig.4. For this value of  $U_S$  the system gets closer to the magnetic instability (though this  $U_S$  is not large enough to stabilize the magnetic order), and the correlation length of  $m$  becomes larger. Then the magnetization  $m$  penetrates far inside the S side compared with Fig.2, and the  $d$ - and  $s$ -wave SCOP's decay rather slowly.

In the  $\mathcal{T}$ -violating SC state a spontaneous current flows along the surface in the region where the SCOP's are spatially varying [19–21]. Note that the condition for the minimum free energy requires the current normal to the interface to vanish. This condition in turn leads to a finite current along the interface if  $\mathcal{T}$  is broken. (Namely the present spontaneous current is the equilibrium current.) The expressions for the currents carried by spin-up and spin-down electrons are given by

$$\begin{aligned} J_y^\uparrow(i) &= -\frac{2eta}{\hbar} \frac{1}{N_y} \sum_{k,n} \sin ka |u_{i,n}(k)|^2 f(E_n(k)) \\ J_y^\downarrow(i) &= \frac{2eta}{\hbar} \frac{1}{N_y} \sum_{k,n} \sin ka |v_{i,n}(k)|^2 [1 - f(E_n(k))]. \end{aligned} \tag{10}$$

Since we do not consider the effect of the vector potential  $\vec{A}$  in this paper, terms linear in  $\vec{A}$  in the expressions of  $J_y$  are not taken into account. Near the surface faced to vacuum only the charge current (defined as  $J_{\text{charge}} = J^\uparrow + J^\downarrow$ ) can flow [22]. When the surface is attached to a ferromagnet,  $m$  is finite in the region where the chiral SCOP's have spatial variations. Thus  $J^\uparrow$  is not equal to  $J^\downarrow$ , and the spontaneous spin current (defined as  $J_{\text{spin}} = J^\uparrow - J^\downarrow$ ) appears as seen in Fig.5(a). For small value of  $t_T (= 0.1)$ , only small spin current flows while the charge current is large (Fig5(b)). This is because the penetration of  $m$  into the S side is suppressed (Fig.3), and then the difference between  $J_\uparrow$  and  $J_\downarrow$  is reduced. When the  $(p_x \pm ip_y)$ -wave superconductor is faced to vacuum, only a charge current arises and no spin current shows up [22]. The  $t_T$ -dependence of spin currents presented here is consistent with this fact. When the effect of electron correlations is important in the S side,  $J_{\text{charge}}$  is reduced but  $J_{\text{spin}}$  is not (Fig.5(c)). This is because a large  $U_S$

suppresses  $\Delta_p$ 's leading to a reduced  $J_{\text{charge}}$ , while it enhances  $m$  and  $J_{\text{spin}}$ . The spin current also becomes larger as the value of  $U_F$  is increased (Fig.5(d) with  $U_F = 16$ ), since  $m$  in the F side is enhanced leading to larger value of  $m$  in the S side. To summarize the discussion of the spin current in bilayer systems,  $J_{\text{spin}}$  can be large if the magnetization induced in the S side is large.

We have also investigated the case of [110] interface between a  $(p_x \pm ip_y)$ -wave superconductor and a ferromagnet, and the results are qualitatively the same as those for the [100] interface.

Now we examine the F/S/F trilayer system where S is a chiral  $(p_x \pm ip_y)$ -wave superconductor. The spatial variations of the magnetization  $m$  and the  $p$ -wave SCOP's are shown in Fig.6. (Small  $\text{Re}\Delta_d$  and  $\text{Re}\Delta_s$  are also induced near the interface as in F/S bilayer system, though they are not shown here.) In the F/S bilayer system, we have seen that spontaneous spin currents as well as charge currents flow along the interface. The direction of the charge current,  $J_{\text{charge}}$ , is determined by the chirality (i.e.,  $(p_x + ip_y)$  or  $(p_x - ip_y)$ ), and the currents at the opposite edges of the superconductor should flow in opposite directions. The direction of the spin current,  $J_{\text{spin}}$ , is the same as (opposite to) that at the other edge of the superconductor if the magnetizations of two ferromagnets are antiparallel (parallel). Then if the chiral superconductor is sandwiched by ferromagnets with antiparallel magnetizations, the total charge current (integrated over  $x$ ) should vanish, while the total spin current will be finite. On the contrary if the magnetization of two F layers are parallel, both the total charge current and the total spin current should vanish. This is actually the case as shown in Fig.7, where  $\sum_i J_{\text{charge}}(i)$  vanishes for both parallel and antiparallel configurations of  $m$  and  $\sum_i J_{\text{spin}}(i)$  is finite only for an antiparallel configuration of  $m$ . If we assume  $t = 1\text{eV}$ ,  $\sum_i J_{\text{spin}}(i) \sim 10\mu\text{A}$ .

#### IV. INTERFACE STATES FOR D-WAVE SUPERCONDUCTORS

In this section we examine the interface states for ferromagnets and superconductors with  $d_{x^2-y^2}$ -wave symmetry. In order to realize the ferromagnetic and the  $d_{x^2-y^2}$ -wave SC states in F and S layers, respectively, the parameters are chosen to be  $U_F = 10$ ,  $U_S = 1.5$ ,  $V_S = -1.5$  and  $\mu = -0.5$ . We consider only the [110] interface here, since a  $\mathcal{T}$ -breaking surface state may be formed in this case, but not in the case of a [100] surface [29]. The  $\mathcal{T}$ -violating surface state can be formed by introducing additional SCOP, such as  $is$  or  $id_{xy}$ -wave component [14]. In the present model ( $d_{x^2-y^2} \pm is$ )-wave state may occur, because the attractive interaction exists between nearest-neighbor sites on a square lattice. (It may be possible to induce  $id_{xy}$  SCOP near the magnetic impurity with spin-orbit interactions or due to the

magnetic field [30,31].) In the  $(d \pm is)$ -wave surface state, the spontaneous charge current flows along the  $y'$  direction. If a ferromagnet is attached to a [110] surface of a  $d_{x^2-y^2}$ -wave superconductor, the coexistence of the magnetization  $m$  in the  $\mathcal{T}$ -violating state may be expected, leading to a spontaneous spin current.

In Fig.8 the spatial variations of  $m$  and the SCOP's near the [110] interface are shown for  $t_T = 0.1$ . Since a  $d_{x^2-y^2}$ -wave SC state has nodes in contrast to a fully gapped  $(p_x \pm ip_y)$ -wave SC state, the proximity effect in the former case is much larger than that in the latter. (See Fig.3 where the same  $t_T = 0.1$  is employed in the case of  $(p_x \pm ip_y)$ -wave superconductor.) When  $t_T$  is not so small ( $t_T \gtrsim 0.02$  for  $U$ 's and  $V$ 's used here), the magnetization penetrates into the S layer (Fig.9). When  $m \neq 0$ , the density of spin-up and spin-down electrons are not equal, and the Cooper pairs cannot be formed in singlet channels only, and thus the  $p$ -wave components have to arise [5]. We find that the complex component ( $is$ ), which could be induced near a surface faced to vacuum, is destroyed, and the resulting state has a  $(d_{x^2-y^2} + p_x + p_y)$ -symmetry. When the value of  $t_T$  is reduced, the symmetry of the SC state changes. For  $t_T \lesssim 0.02$ ,  $(d \pm is)$ -wave state appears, where the magnetization  $m$  (and thus  $p$ -wave SCOP's) is absent in the S layer even though  $t_T \neq 0$ . (Fig.10)

In the  $(d \pm is)$ -state a spontaneous charge current can flow along the interface, but there is no spin current because  $m = 0$ . In the  $(d + p_x + p_y)$ -state both charge and spin current vanish, because all SCOP's are real. (Fig.11) For the [110] interface the expression for the current  $J_{y'}^\sigma(i)$  is slightly different from that for [100] case. We checked that the current from the site  $i$  to  $i + \hat{x}'/2 + \hat{y}'/2$ , denoted as  $J_a^\sigma(i)$ , is the same as that from the site  $i + \hat{x}'/2 + \hat{y}'/2$  to  $i + \hat{y}'$ , denoted as  $J_b^\sigma(i)$ . (Otherwise  $J_{x'}^\sigma(i) \neq 0$ .) Then  $J_{y'}^\sigma(i)$  is given by the  $y'$  component of  $J_a^\sigma(i)$  (or, equivalently  $J_b^\sigma(i)$ ):

$$\begin{aligned} J_{y'}^\uparrow(i) &= \frac{1}{\sqrt{2}} \frac{2et_i a}{\hbar} \frac{1}{N_{y'}} \sum_{k,n} f(E_n(k)) \times \\ &\quad \text{Im}[u_{i+\frac{a'}{2},n}^*(k) u_{i,n}(k) e^{-ika'/2}] \\ J_{y'}^\downarrow(i) &= \frac{1}{\sqrt{2}} \frac{2et_i a}{\hbar} \frac{1}{N_{y'}} \sum_{k,n} [1 - f(E_n(k))] \times \\ &\quad \text{Im}[v_{i+\frac{a'}{2},n}(k) v_{i,n}^*(k) e^{ika'/2}]. \end{aligned} \tag{11}$$

where  $t_i = t_T$  if  $i$  corresponds to the interface site,  $t_i = t$  otherwise.

The transition between the  $(d \pm is)$ - and  $(d + p_x + p_y)$ -wave SC states is of first order, and we did not find a state which carries a spontaneous spin current for F/S( $d_{x^2-y^2}$ ) interface states. Our results imply that both the state with  $m \neq 0$ ,  $\Delta_s = 0$  and  $\Delta_{px(y)} \neq 0$ , and the state with  $m = 0$ ,  $\Delta_s \neq 0$  and  $\Delta_{px(y)} = 0$  correspond to the local minima of the free energy, and that the former (latter)

has lower energy when  $t_T > (t_T)_{cr}$  ( $t_T < (t_T)_{cr}$ ) with  $(t_T)_{cr} \sim 0.02$ . Actually for  $t_T \sim (t_T)_{cr}$ , we obtained two kinds of solutions depending on the initial values of OP's for the iteration, and the energies of two solutions cross at  $t_T = (t_T)_{cr}$ .

## V. SUMMARY

We have studied the proximity effect between unconventional superconductors and ferromagnets. It is found that a spontaneous spin current can flow along the interface between a  $(p_x \pm ip_y)$ -wave superconductor and a ferromagnet due to the coexistence of the magnetization and the chiral superconducting state. In the case of a  $d_{x^2-y^2}$ -wave superconductor the induced magnetization destroys the  $\mathcal{T}$ -breaking ( $d \pm is$ )-wave surface state for relatively large transmission ( $t_T \gtrsim 0.02$ ). For small transmission ( $t_T \lesssim 0.02$ ) the ( $d \pm is$ )-wave SC state with  $m = 0$  is realized, and we did not find the state with a spontaneous spin current for any value of  $t_T$ . This implies that only a spontaneous charge current may be possible for high- $T_c$  cuprates, while both spin and charge currents may be expected for spin-triplet superconductors, e.g.,  $\text{Sr}_2\text{RuO}_4$ . For conventional  $s$ -wave superconductors based on the electron-phonon mechanism, the ferromagnetism plays a very strong role to suppress the superconductivity. On the contrary, in the case of unconventional superconductors these effects may be weaker, since the superconductivity is caused by the magnetic interactions. Then we expect it is possible to obtain a surface state with a spontaneous spin current experimentally using spin-triplet superconductors.

## ACKNOWLEDGMENT

The authors are grateful to G. Tatara, H. Kohno, M. Sigrist, H. Shiba and H. Fukuyama for useful discussions. This work was financially supported by Sumitomo foundation.

- 
- [1] R. Meservey and P.M. Tedrow, Phys. Rep. **238**, 173 (1994).
  - [2] S. Kashiwaya and Y. Tanaka, Rep. Prog. Phys. **63**, 1641 (2000).
  - [3] E. Demler, A. J. Berlinsky, C. Kallin, G. B. Arnold and M. R. Beasley: Phys. Rev. Lett. **80**, 2917 (1998).
  - [4] J.X. Zhu, B. Friedman and C.S. Ting, Phys. Rev. B **59**, 9558 (1999).
  - [5] K. Kuboki, J. Phys. Soc. Jpn. **68**, 3150 (1999).
  - [6] J.X. Zhu and C.S. Ting, Phys. Rev. B **61**, 1456 (2000).

- [7] M.H.S. Amin et al., Phys. Rev. B **63**, 212502 (2001).
- [8] M.H.S. Amin et al., Phys. Rev. B **66**, 174515 (2002).
- [9] F.S. Bergeret et al., Phys. Rev. Lett., **86**, 4096 (2001).
- [10] A.F. Volkov et al., Phys. Rev. Lett., **90**, 117006 (2003).
- [11] F.S. Bergeret et al., Phys. Rev. B **69**, 174504 (2004).
- [12] D. Scalapino: Phys. Rep. **250**, 329 (1995).
- [13] T.M. Rice and M. Sigrist, J. Phys. Condens. matter **7**, L643 (1995).
- [14] For a review on  $T$ -breaking SC states, see for example, M. Sigrist, Prog. Theor. Phys. **99**, 899 (1998).
- [15] M. Sigrist, D.B. Bailey and R.B. Laughlin, Phys. Rev. Lett., **74**, 3249 (1995).
- [16] K. Kuboki and M. Sigrist: J. Phys. Soc. Jpn. **65**, 361 (1996); cond-mat/9501029.
- [17] M. Matsumoto and H. Shiba: J. Phys. Soc. Jpn. **64**, 3384 (1995); *ibid.* **64**, 4867 (1995).
- [18] M. Fogelström, D. Rainer, and J. A. Sauls, Phys. Rev. Lett. **79**, 281 (1997).
- [19] G.E. Volovik and L.P. Gorkov, Zh. EKsp. Teor. Fiz. **88**, 1412 (1985) [Sov. Phys. JETP **61**, 843 (1985)].
- [20] M. Sigrist, T.M. Rice and K. Ueda: Phys. Rev. Lett. **63**, 1727 (1989)
- [21] For a review see M. Sigrist and K. Ueda, Rev. Mod. Phys., **63**, 239 (1991).
- [22] M. Matsumoto and M. Sigrist, J. Phys. Soc. Jpn. **68**, 994 (1999).
- [23] A preliminary result was already published in; K. Kuboki and H. Takahashi, Physics B **329-333**, 1440 (2003).
- [24] M. Krawiec et al., Phys. Rev. B **66**, 172505 (2002).
- [25] See e.g., P.G. de Gennes: *Superconductivity of Metals and Alloys* (Addison-Wesley,1989).
- [26] J. E. Hirsch, Phys. Rev. B **31**, 4403 (1985).
- [27] R. Micnas, J. Ranninger and S. Robaszkiewicz: Rev. Mod. Phys. **62**, 113 (1990).
- [28] K. Kuboki, J. Phys. Soc. Jpn. **70**, 2698 (2001).
- [29] The [110] magnetically ordered surface state faced to vacuum was studied in, C. Honerkamp, K. Wakabayashi and M. Sigrist, Europhysics Lett. (France) **50**, 368 (2000).
- [30] A.V. Balatsky, Phys. Rev. Lett., **80**, 1972 (1998).
- [31] R.B. Laughlin, Phys. Rev. Lett., **80**, 5188 (1998).

**Fig. 1** Schematic descriptions of the interfaces between ferromagnets and superconductors for (a) [100] and (b) [110] surfaces.

**Fig. 2** Spatial variations of the magnetization  $m$  and the SCOP's for a F/S( $p_x + ip_y$ ) bilayer system with  $t_T = 1$ ,  $U_F = 12$ ,  $U_S = 1.5$ ,  $V_S = -2.5$ ,  $\mu = -1.6$ ,  $N_x = 60 + 60$  and  $N_y = 120$ . (a)  $m$ , (b)  $\text{Re}\Delta_{px}$ , (c)  $\text{Im}\Delta_{py}$ , (d)  $\text{Re}\Delta_d$  and (e)  $\text{Re}\Delta_s$ . Note all OP's are non-dimensional, and  $x = 0$  corresponds to the interface site of a ferromagnet.

**Fig. 3** Spatial variations of  $m$  and the SCOP's for a F/S( $p_x + ip_y$ ) bilayer system with  $t_T = 0.1$ . Other parameters are the same as in Fig.2. (a)  $m$ , (b)  $\text{Re}\Delta_{px}$ , (c)  $\text{Im}\Delta_{py}$ , (d)  $\text{Re}\Delta_d$  and (e)  $\text{Re}\Delta_s$ .

**Fig. 4** Spatial variations of  $m$  and the SCOP's for a F/S( $p_x + ip_y$ ) bilayer system with  $U_S = 5$ . Other parameters are the same as in Fig.2. (a)  $m$ , (b)  $\text{Re}\Delta_{px}$ , (c)  $\text{Im}\Delta_{py}$ , (d)  $\text{Re}\Delta_d$  and (e)  $\text{Re}\Delta_s$ .

**Fig. 5** The charge and the spin current (in units of  $2eta/\hbar$ ) for F/S( $p_x + ip_y$ ) bilayer systems. (a)  $U_F = 12$ ,  $U_S = 1.5$  and  $t_T = 1$ , (b)  $U_F = 12$ ,  $U_S = 1.5$  and  $t_T = 0.1$ , (c)  $U_F = 12$ ,  $U_S = 5$  and  $t_T = 1$  and (d)  $U_F = 16$ ,  $U_S = 1.5$  and  $t_T = 1$ . Other parameters are the same as in Fig.2.

**Fig. 6** Spatial variations of  $m$ ,  $\text{Re}\Delta_{px}$  and  $\text{Im}\Delta_{py}$  for F/S( $p_x + ip_y$ )/F trilayer systems. The system size is  $N_x = 40 + 40 + 40$ ,  $N_y = 120$ , and other parameters are the same as in Fig.2. (a)  $m$  with parallel configuration, (b)  $m$  with antiparallel configuration in two F layers, respectively. (c)  $\text{Re}\Delta_{px}$  and (d)  $\text{Im}\Delta_{py}$ . Note  $\text{Re}\Delta_{px}$  and  $\text{Im}\Delta_{py}$  do not depend on the configurations of  $m$ .

**Fig. 7** The charge and the spin current (in units of  $2eta/\hbar$ ) for F/S( $p_x + ip_y$ )/F trilayer systems. Parameters used are the same as in Fig.6. Magnetization of two F layers are antiparallel in (a), and parallel in (b).

**Fig. 8** Spatial variations of  $m$  and the SCOP's for a F/S( $d_{x^2-y^2}$ ) bilayer system with  $t_T = 0.1$ ,  $U_F = 10$ ,  $U_S = 1.5$ ,  $V_S = -1.5$ ,  $\mu = -0.5$ ,  $N_{x'} = 60 + 60$  and  $N_{y'} = 120$ . (a)  $m$ , (b)  $\text{Re}\Delta_d$  and (c)  $\text{Re}\Delta_{px}(= \text{Re}\Delta_{py})$ .

**Fig. 9** Spatial variations of  $m$  and the SCOP's for a F/S( $d_{x^2-y^2}$ ) bilayer system with  $t_T = 0.03$ . Other parameters are the same as in Fig.8. (a)  $m$ , (b)  $\text{Re}\Delta_d$  and (c)  $\text{Re}\Delta_{px}(= \text{Re}\Delta_{py})$ .

**Fig. 10** Spatial variations of  $m$  and the SCOP's for a F/S( $d_{x^2-y^2}$ ) bilayer system with  $t_T = 0.01$ . Other parameters are the same as in Fig.8. (a)  $m$ , (b)  $\text{Re}\Delta_d$  and (c)  $\text{Im}\Delta_s$ .

**Fig. 11** The charge current (in units of  $2eta/\hbar$ ) for F/S( $d_{x^2-y^2}$ ) bilayer systems with (a)  $t_T = 0.1$  and  $t_T = 0.03$ , and (b)  $t_T = 0.01$ . Other parameters are the same as in Fig.8.

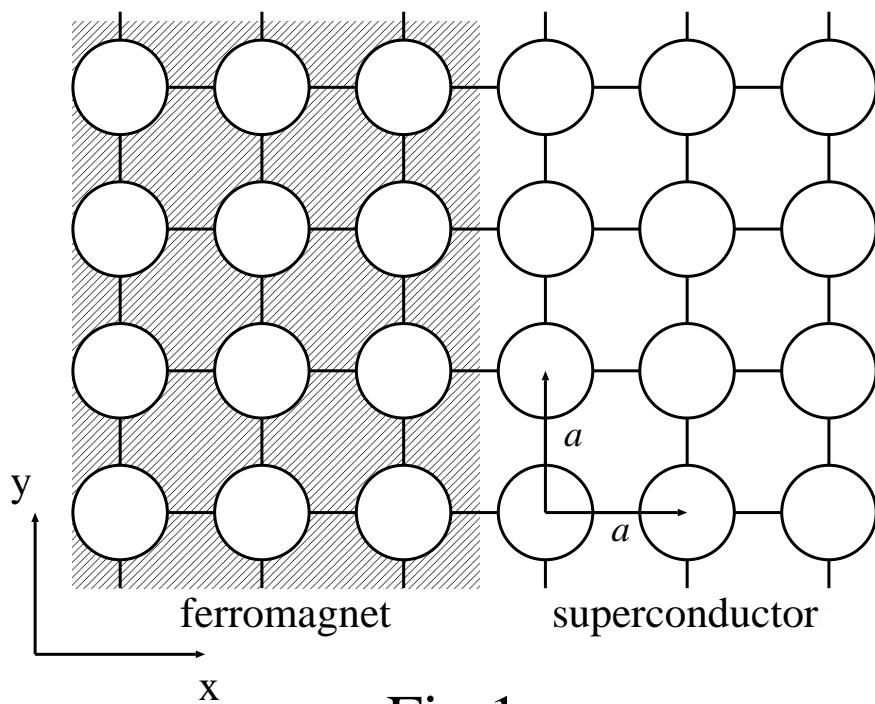


Fig.1a

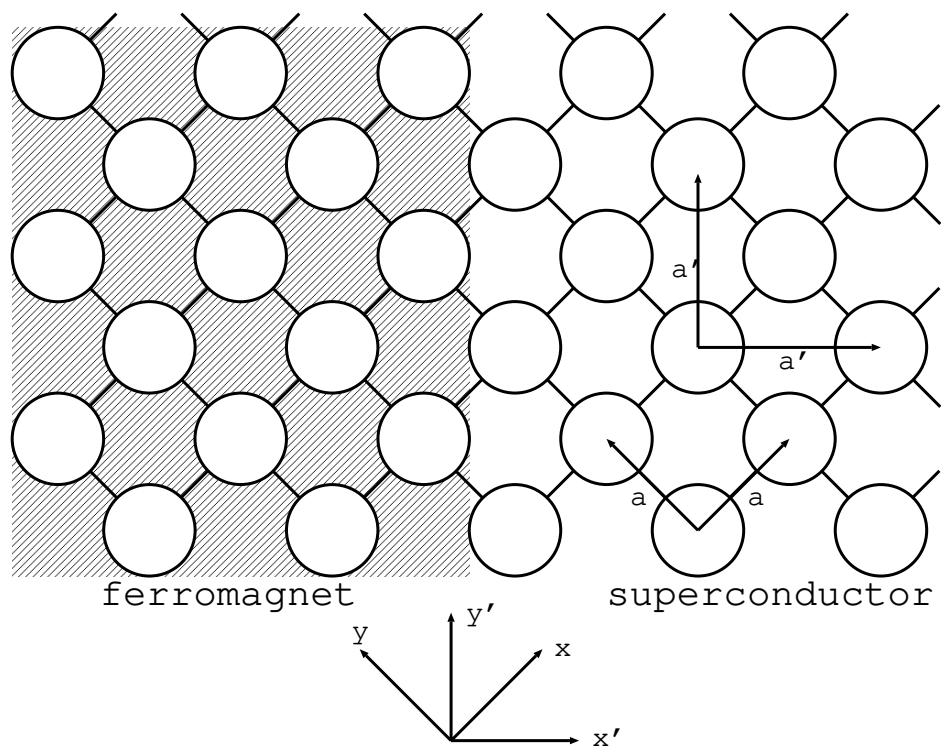


Fig.1b

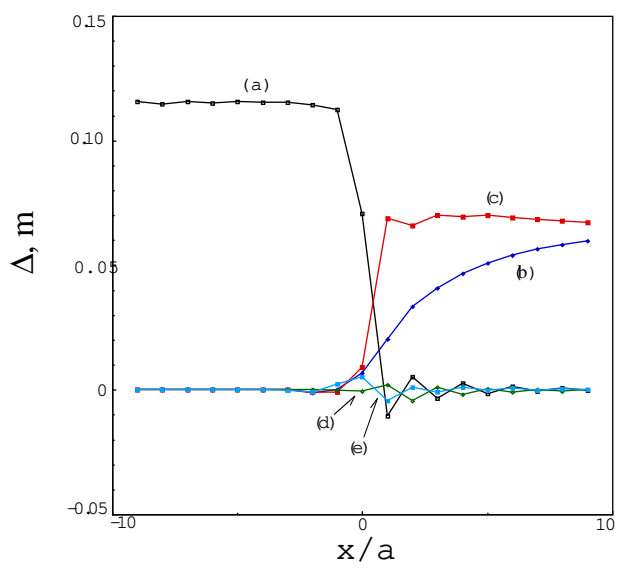


Fig.2

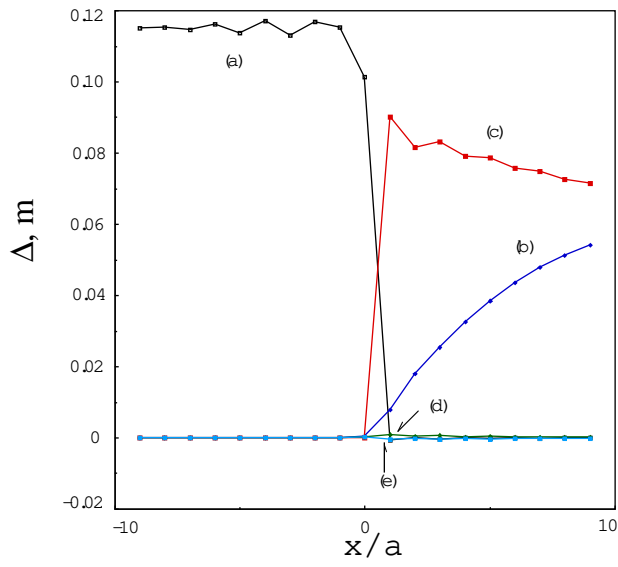


Fig.3

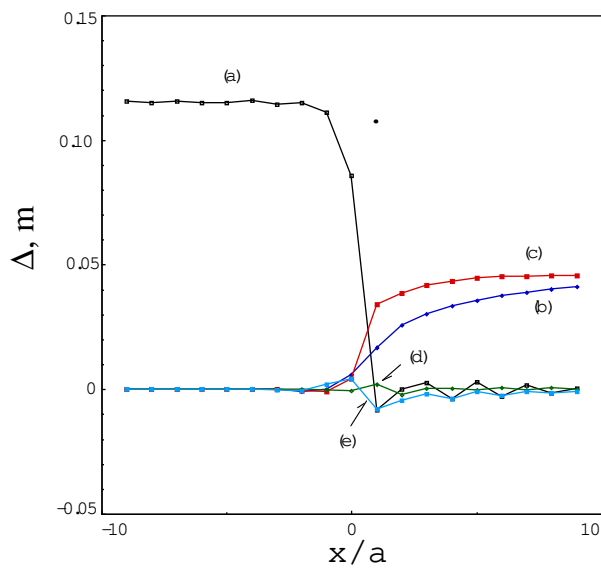
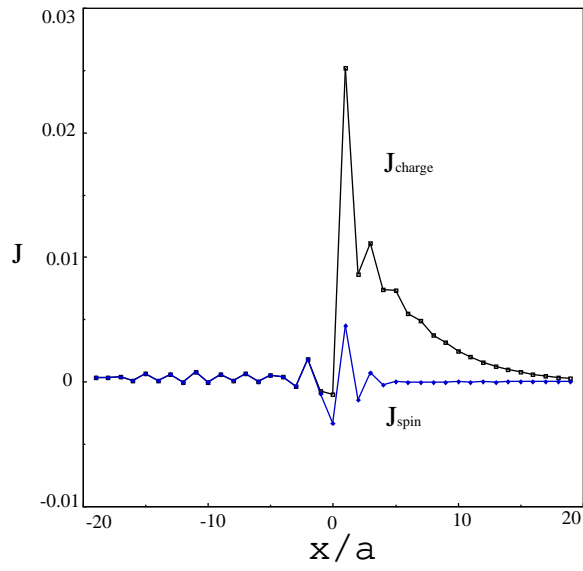
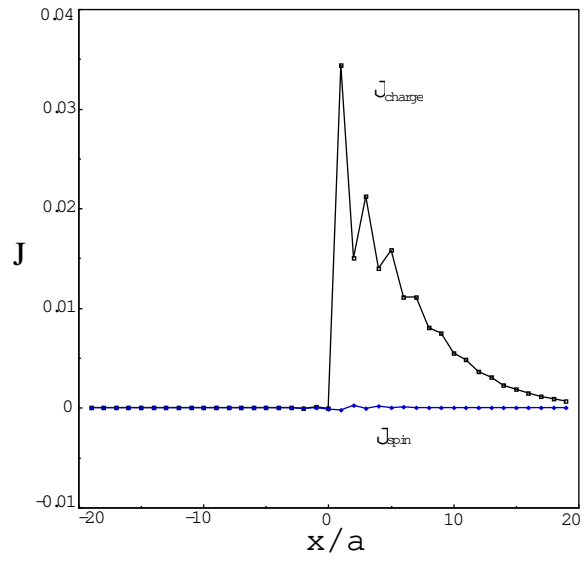


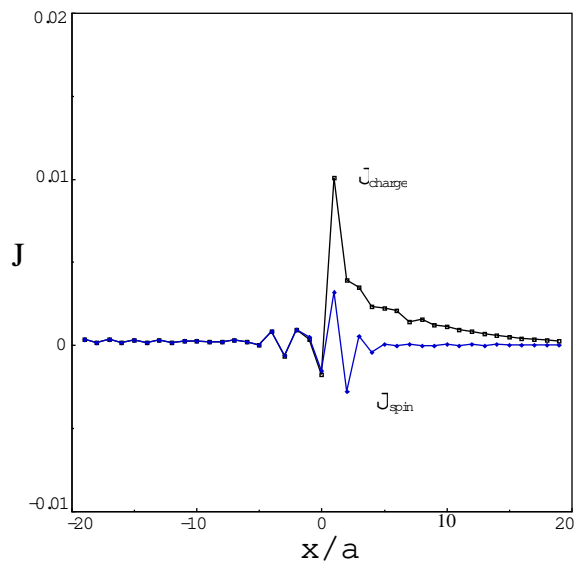
Fig.4



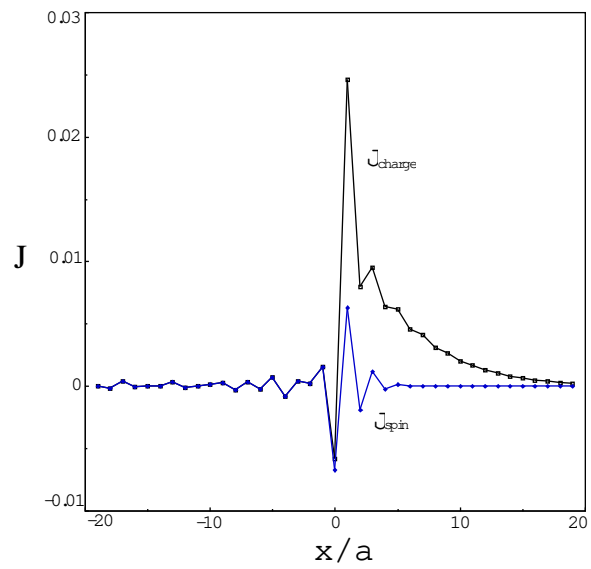
(a)



(b)



(c)



(d)

Fig.5

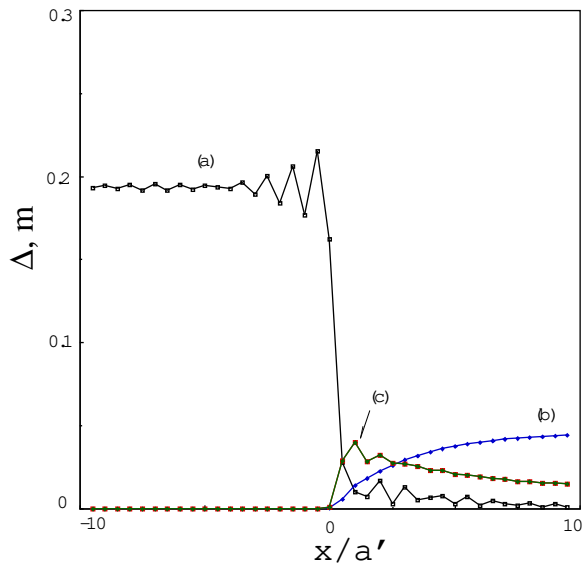


Fig.8

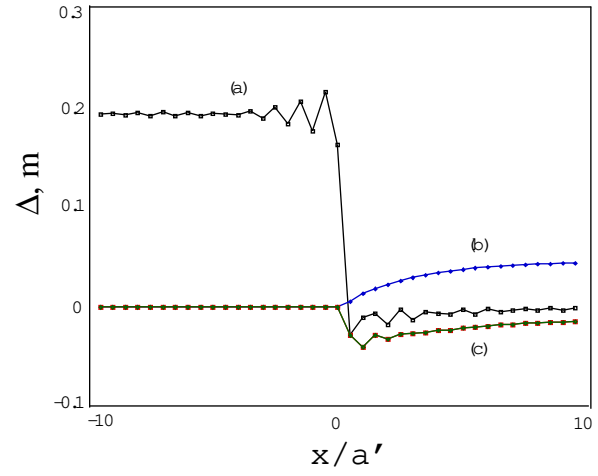


Fig.9

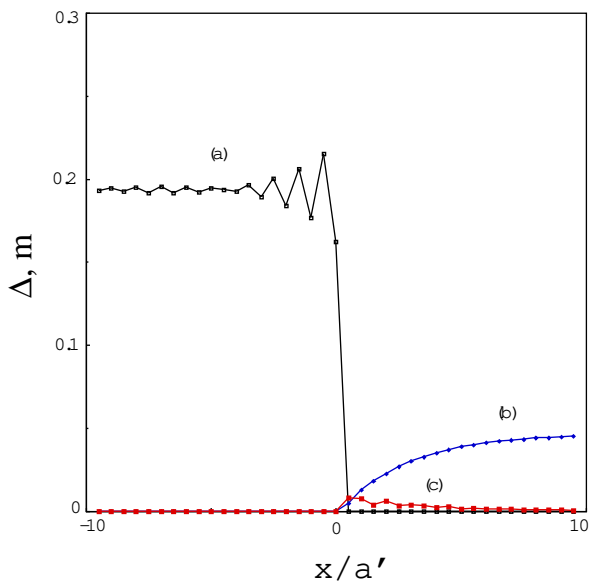


Fig.10

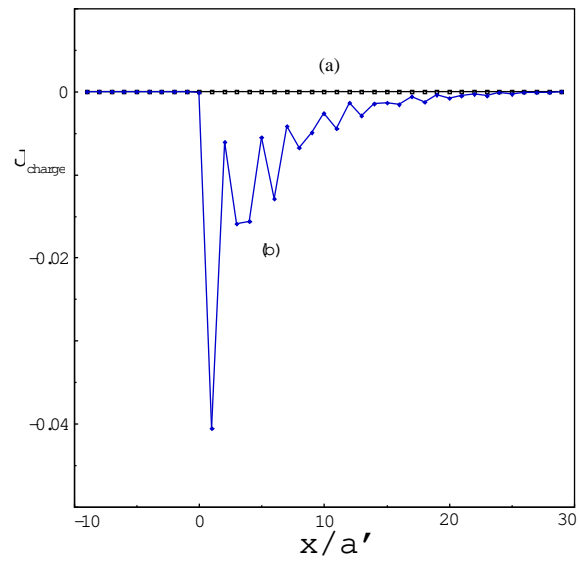


Fig.11

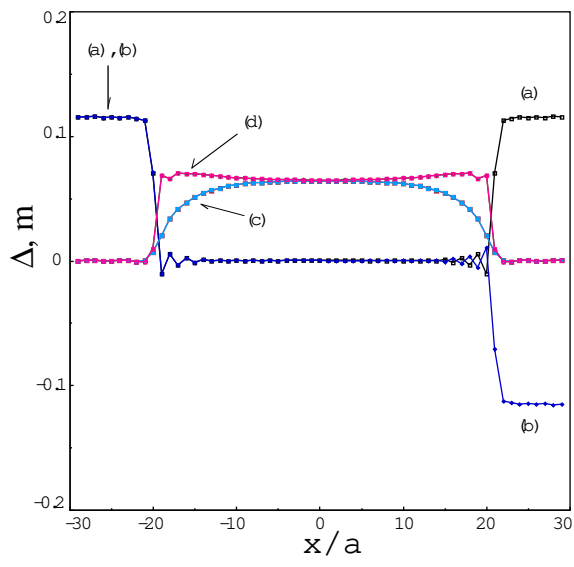


Fig.6

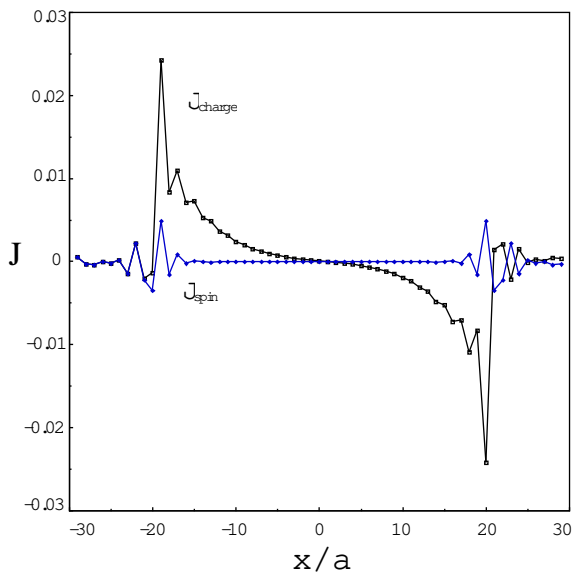


Fig.7(a)

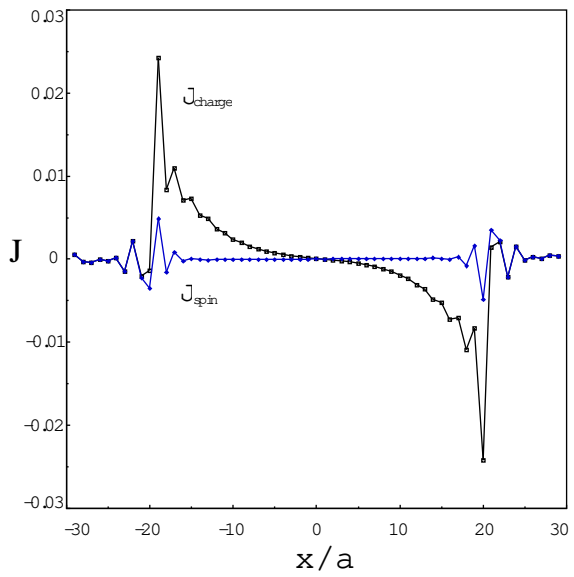


Fig.7(b)